



Full waveform inversion with well control

Babatunde Arenrin, CREWES, University of Calgary, Gary Margrave, CREWES, University of Calgary, John Bancroft, University of Calgary*

Summary

This report presents the application of full waveform inversion with well control on Hussar synthetics. In this study, we present the result obtained from incorporating well log information into a conjugate gradient optimization scheme in Full Waveform Inversion (FWI). We test this approach on synthetic datasets generated using the three sonic logs from Hussar. Using formation tops to guide the interpolation, the sonic logs are interpolated to form the 2D velocity model used in this study. The initial velocity models for the inversion are a linear $v(z)$ velocity model and also a smooth version of the true model. We adopt the conjugate gradient algorithm as described by Magnus R. Hestenes and Eduard Stiefel. Our results show that combining well information with conjugate gradient directions in FWI can save computational time, speed up convergence rate, as well as getting a good inverted model after a few iterations. The inverted model is encouraging which proves that our algorithm works well and can resolve the thin layers in the true model.

Introduction

Full waveform inversion is an optimization technique that seeks to find a model of the subsurface that best matches the recorded field data at every receiver location. The method begins from a best guess of the true model, which is iteratively improved using linearized inversions methods. FWI is formulated as a generalised inverse problem with a numerical solver—a forward modelling code and its adjoint. FWI can be viewed as an iterative cycle involving modelling, pre-stack migration and velocity model updating in each iteration (Margrave et al, 2010).

Despite its success, FWI suffers from cycle skipping problems, and convergence problems when the starting model is far from the true model and in the absence of low frequencies. However different approaches have been developed to mitigate the problems with conventional FWI, such as incorporating well information to FWI (Margrave et al, 2011a). Well information can aid in (1) calculating the step-length (a scalar which multiplies the gradient for the model update), (2) constraining the line search calculation used in a steepest descent optimization scheme, and (3) improving the wavelet estimate which is essential for proper updates. Some other approaches that mitigate the problems with conventional FWI are Tomographic Full waveform Inversion (TFWI) which combines both FWI and WEMVA (Biondi and Almomin, 2012), and Adaptive Waveform Inversion (AWI) in which the observed and predicted datasets are matched trace-by-trace using a least squares convolutional filter (Warner and Guasch, 2014).

In previous papers (Arenrin et al, 2014 and Arenrin et al, 2015), we compared using well log derived step length with a line search optimization scheme, and found that deriving step lengths based on well information produced good inversion results. In that paper, we also proposed that a combination of step lengths derived based on well information with any type of optimization scheme should produce desirable results than using either method only. In this report, we combine well information with conjugate gradient optimization scheme and obtain encouraging results within a few iterations. In an optimization algorithm, such as the steepest descent method, the scalar (step length) can be calculated using a line search algorithm or if there is well control, a method based on well information.

The scalar calculated using well information compares the current velocity model to that of the known velocity at the well location. We define an objective function β which is the L2 norm of the difference between the model update calculated from migrating the data residuals and the known velocity at the well and the background velocity model expressed as,

$$\beta = \left\| \lambda G_k - (V_{well} - V_{BG})_k \right\|^2 \quad (1)$$

where G_k is the migration of the data residuals stacked over all shots at the well location, V_{well} is the known velocity at the well location, V_{BG} is the background velocity (or the migration velocity) at the well location, and the L2 norm is taken over all the samples in the well (with real data it is necessary to resample the well information to the same sample density as the migration velocity model).

The scalar λ is obtained by minimizing the objective function β in Equation 1 with respect to λ . Making λ the subject of the expression gives,

$$\lambda = \frac{\sum_j \delta V_j G_j}{\sum_j G_j^2} \quad (2)$$

where $\delta V_j = (V_{well} - V_{BG})_j$ and j indicates sample number.

Method

Conjugate gradient (CG) method based on Magnus R. Hestenes and Eduard Stiefel

The history and theory of conjugate gradient methods can be found in several literatures, however, we will just present one of the conjugate gradient algorithm described by Hestenes and Stiefel, 1952. We notice that this conjugate gradient algorithm in geophysical papers is often credited to Polak and Ribiere, and is known as the Polak-Ribiere method. However, we found the same algorithm in Hestenes and Stiefel 1952 paper which predates Polak and Ribiere's 1969 paper. The conjugate gradient is an iterative method that starts with an initial estimate of the solution, and one determines successively new estimates of the solution, each estimate being closer to the true solution (Hestenes and Stiefel, 1952). The algorithm can be summarised thus:

$\alpha_{k-1} = \frac{ \nabla \phi_{k-1} ^2}{(p_{k-1}, Ap_{k-1})}$	$\alpha_{k-1} = \frac{ \nabla \phi_{k-1} ^2}{(p_{k-1}, Ap_{k-1})}$	$\lambda_{k-1} = \frac{\sum_j \delta V_j G_j}{\sum_j G_j^2}$
$v_k = v_{k-1} + \alpha_{k-1} p_{k-1}$	$v_k = v_{k-1} + \alpha_{k-1} p_{k-1}$	$v_k = v_{k-1} + \lambda_{k-1} p_{k-1}$
$\beta_k = \frac{ \nabla \phi_k ^2 - (\nabla \phi_k, \nabla \phi_{k-1})}{ \nabla \phi_{k-1} ^2}$	$\beta_k = \frac{ \nabla \phi_k ^2 - (\nabla \phi_k, \nabla \phi_{k-1})}{ \nabla \phi_{k-1} ^2}$	$\beta_k = \frac{ \nabla \phi_k ^2 - (\nabla \phi_k, \nabla \phi_{k-1})}{ \nabla \phi_{k-1} ^2}$
$p_k = \nabla \phi_k + \beta_k p_{k-1},$	$p_k = (1 + \beta_k)^{-1} (\nabla \phi_k + \beta_k p_{k-1}),$	$p_k = (1 + \beta_k)^{-1} (\nabla \phi_k + \beta_k p_{k-1}),$

Figure 1: Left: Hestenes and Stiefel CG algorithm (Hestenes and Stiefel, 1952), centre: Hestenes modified CG algorithm (Hestenes, 1990), right: the modified CG algorithm used in this study by incorporating well information.

where $\nabla\phi$ and p_k are the gradient of the objective function and the conjugate direction respectively. β_k is designed to guarantee that p_k and p_{k-1} are conjugate, k is the iteration number, while α_{k-1} or λ_{k-1} (calculated using Equation 2 at each iteration) acts to scale the conjugate direction p_{k-1} .

Examples

We test this algorithm on synthetic datasets generated from the three sonic logs from Hussar. By interpolating between the logs we obtain a 2-D velocity model that is used to generate synthetic datasets. The interpolation between the logs was guided by the formation tops. The datasets are generated using an acoustic finite difference forward modelling code. We test our algorithm using different starting models for the inversion: a linear $v(z)$ velocity model, and a slightly smooth version of the true model.

Modelling and Migration (inversion)

Fig 7 below is the 2-D velocity model obtained from the interpolation of the three logs from Hussar. Wells 14-35, 14-27, and 12-27 are superimposed on the velocity model. One can observe the fine stratigraphy and notice that the interpolation was guided by the formation tops as evident on the character of the logs. The 2-D velocity model is about 4km wide and 2Km deep, described by approximately 1.3×10^6 discrete parameters. A total of 61 shots is generated with the acoustic finite-difference code, with a shot spacing of about 67 meters, receiver spacing is 2.5 meters, sampling interval is 2ms, and a total of 1600 receivers. The source wavelet is minimum wavelet with a dominant frequency of 50 hertz. All boundaries for both the modelling and migration are absorbing except at the ground-air interface.

For the migration, we use a reverse time migration (RTM) algorithm provided by Acceleware. The RTM algorithm produces a crosscorrelation Imaging Condition (IC) reflectivity image, with the source illumination. With proper pre-conditioning, the source illumination is used to produce the reflectivity image that would have otherwise been obtained if a deconvolution IC had been used. However in this paper we use the crosscorrelation reflectivity image normalised by the source illumination for the gradient calculation.

Conclusions

We have been able to incorporate well information into FWI using a slightly modified CG algorithm originally developed by Hestenes and Stiefel. Our algorithm works well and we have been able to reduce the number of iterations needed for convergence (in comparison to incorporating well information in a steepest descent optimization scheme from our previous papers). This means that the more advanced the optimization algorithm is, the faster will be the rate of convergence by incorporating well information. In the case of using a linear $v(z)$ velocity function, we were able to reach convergence in 9 iterations. A linear $v(z)$ velocity function is not the best starting model for FWI, however, we observe that our algorithm is able to resolve the thin beds and also resolve the area of interest just above the basement rock. In the case of using a smooth version of the velocity model as the starting model, we obtain a high resolution inverted model after 8 iterations. The thin beds are resolved, and the area of interest can be clearly seen. Our algorithm will be tested on some real data in the future.

Acknowledgements

We thank the sponsors of CREWES for their support. We also gratefully acknowledge support from NSERC (Natural Science and Engineering Research Council of Canada) through the grant CRDPJ 461179-13. We thank Acceleware for their contribution.

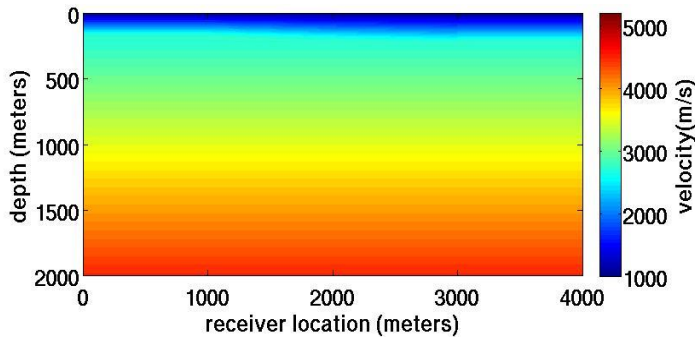


Fig 1. Initial model (linear velocity function).

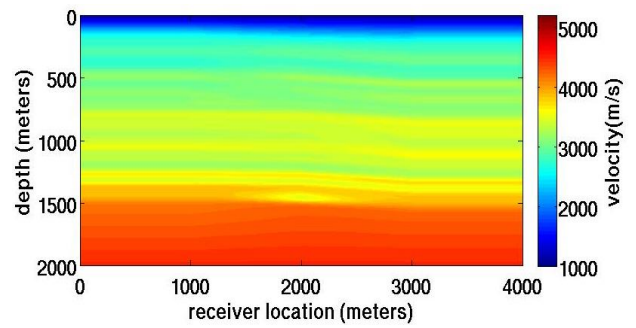


Fig 2. Initial model (smooth velocity function).

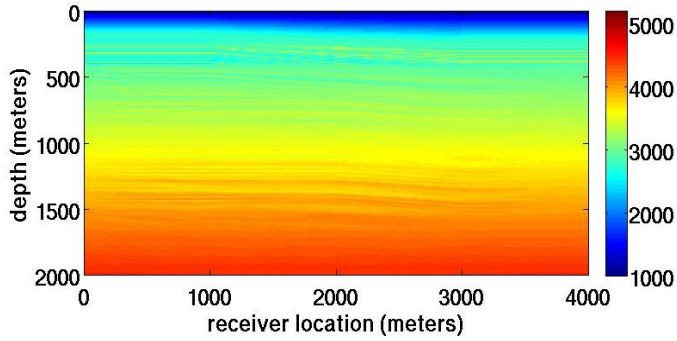


Fig 3. Inverted model after 9 iterations.

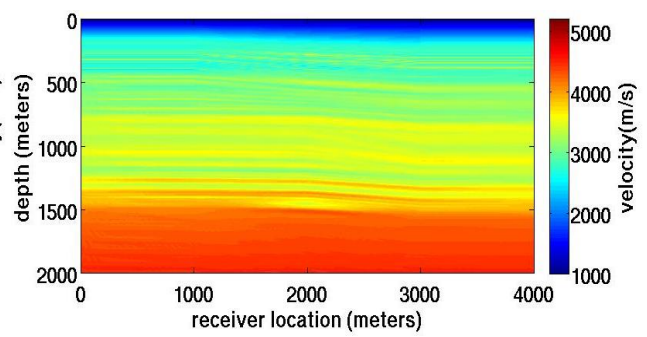


Fig 4. Inverted model after 8 iterations.

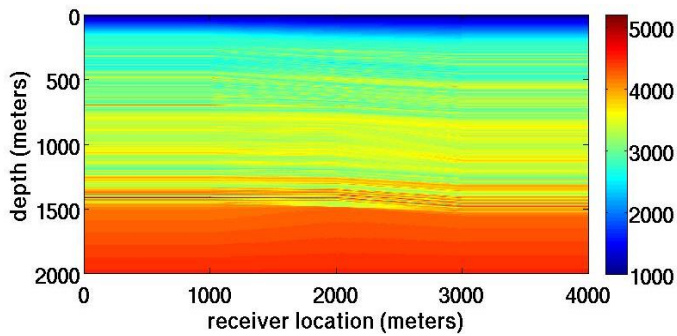


Fig 5. True velocity model.

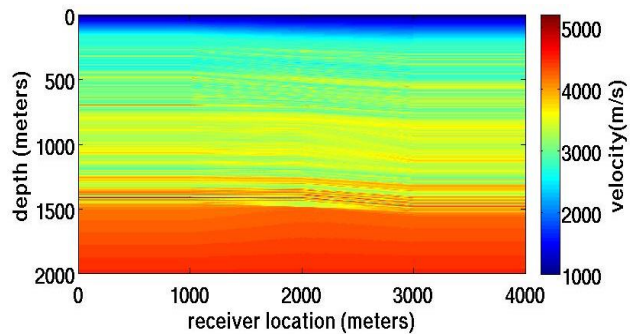


Fig 6. True velocity model.

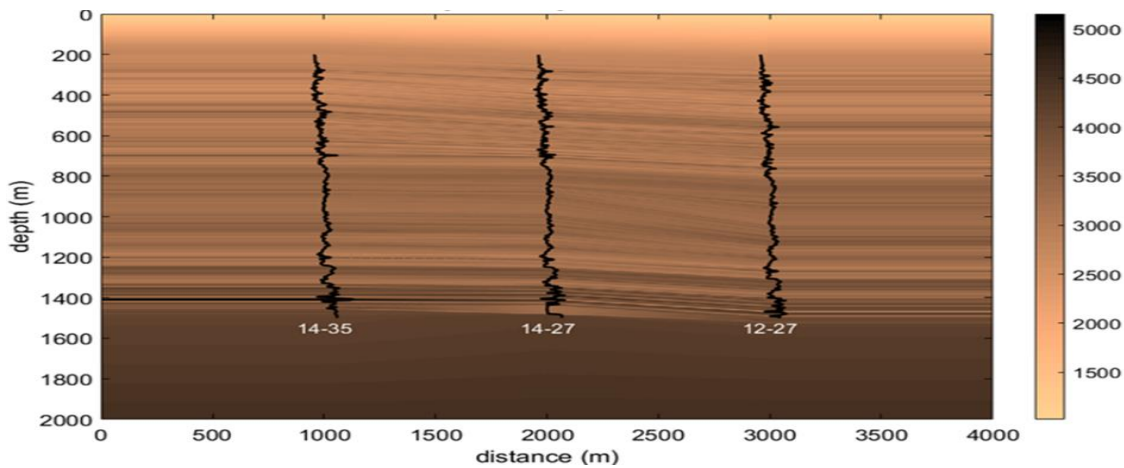


Fig 7. Hussar 2D velocity model interpolated from the three well logs shown in black.

References

Arenrin, B., Margrave, G.F., 2015, Full waveform inversion of Hussar synthetics, in the 27th Annual Research Report of the CREWES Project.

Arenrin, B., Margrave, G.F., and Bancroft, J., 2015, Comparing step length calculation using well logs with a line-search method, CSEG GeoConvention 2015

Arenrin, B., Margrave, G.F., and Bancroft, J., 2014, FWI with source illumination: A synthetic case study in the 26th Annual Research Report of the CREWES Project.

Biondi, B., Almomin, A., 2012; Tomographic full waveform inversion (TFWI) by combining full waveform inversion with wave equation migration velocity analysis, SEG Technical Program Extended Abstracts, 1-5.

Hestenes, M. R., Conjugacy and Gradients, 1990, "A History of Scientific Computing," Stephen G. Nash, editor, pp. 167-179.

Hestenes, M. R., and Stiefel, E., 1952, Methods of Conjugate Gradients for Solving Linear Systems, Journal of Research of the National Bureau of Standard, Vol. 49, 2379,409-436.

Lailly, P., 1983, The seismic inverse problem as a sequence of before stack migrations: Conference on Inverse Scattering, Theory and Application, Society of Industrial and Applied Mathematics, Expanded Abstracts, 206-220.

Margrave, G. F., Ferguson, R. J., and Hogan, C. M., 2010, Full waveform inversion with wave equation migration and well control: in the 22nd Annual Research Report of the CREWES Project.

Margrave, G. F., K. Innanen, and M. Yedlin, 2011a, Full waveform inversion and the inverse Hessian: in the 23rd Annual Research Report of the CREWES Project.

Warner, M., Guasch, L., 2014; Adaptive waveform inversion, SEG Technical Program Extended Abstracts, 1089-1093